MOLECULAR AND CELLULAR BIOLOGY, Nov. 2003, p. 7525–7530 Vol. 23, No. 21
0270-7306/03/$08.00+0 DOI: 10.1128/MCB.23.21.7525–7530.2003

Accelerated Fat Absorption in Intestinal Alkaline Phosphatase Knockout Mice†

Sonoko Narisawa,[1] Lei Huang,[1] Arata Iwasaki,[1] Hideaki Hasegawa,[2] David H. Alpers,[3] and José Luis Millán[1]*

The Burnham Institute, La Jolla, California 92037,[1] Laboratories for Structure and Function Research, Tokai University School of Medicine, Kanagawa, Japan,[2] and Department of Medicine, Washington University School of Medicine, St. Louis, Missouri 63110[3]

Received 5 February 2003/Returned for modification 10 April 2003/Accepted 23 July 2003

Intestinal alkaline phosphatase (IAP) is the most ancestral of the tissue-specific members of the AP gene family. Several studies have suggested an absorptive function for IAP, but in vivo data to this effect have been lacking. We inactivated the mouse IAP gene in embryo-derived stem cells and generated mice homozygous for the null mutation. The mice were macroscopically and histologically normal and fertile and showed no difference from the wild-type controls under normal laboratory conditions. However, when maintained long-term on a high-fat diet, the IAP-deficient mice showed faster body weight gain than did control animals. Histological examination revealed an accelerated transport of fat droplets through the intestinal epithelium and elevation of serum triglyceride levels in the IAP-deficient mice compared to wild-type mice. Our study suggests that IAP participates in a rate-limiting step regulating fat absorption.

Alkaline phosphatases (EC 3.1.3.1) (APs) are dimeric enzymes present in most, if not all, organisms (22). They catalyze the hydrolysis of phosphomonoesters with release of inorganic phosphate and alcohol (22). In humans, three of the four AP isozymes are tissue specific, i.e., the intestinal AP (IAP), placental AP, and germ cell AP, while the fourth AP gene is the tissue-nonspecific AP (TNAP) found expressed in bone, liver, and kidney (12). Mice have the TNAP gene and two tissue-specific APs, i.e., embryonic AP (EAP) and IAP, while the fourth locus is a pseudogene (21).

Gene knockout (KO) experiments have provided unique insights into the biological functions of APs. Inactivation of the mouse TNAP gene phenocopies the human inborn error of metabolism known as infantile hypophosphatasia, characterized by rickets and osteomalacia; epileptic seizures; and increased levels of inorganic pyrophosphate, pyridoxal-5′-phosphate, and phosphoethanolamine (9, 24, 30). It is clear that the epileptic seizures and apnea are due to deficient utilization of pyridoxal-5′-phosphate by TNAP-deficient tissues (26, 30). The bone abnormalities are clearly due to the lack of inorganic pyrophosphatase activity in the cartilage and bone of TNAP KO mice, which are unable to properly regulate the extracellular concentrations of this mineralization inhibitor (13). The EAP gene is the mouse ortholog of human placental AP and germ cell AP (11, 21, 25). Inactivation of the mouse EAP gene appears to have no adverse consequences, and the mice are fertile and live a normal life (25) despite the fact that embryos display a 12-h delay in their preimplantation development (2).

IAP, as the name implies, is expressed in the small intestine of many species. Levels of IAP in lymph and serum increase after a fatty meal (10, 23). Most of our understanding of IAP function is derived from studies of rats, where IAP is found associated with the brush border of the intestinal epithelium, with the highest levels in the duodenum, especially the duodenal crypt and villous cells (14, 31). IAP is enriched in surfactant-like particles (SLP) (3, 7) that appear to be secreted in two directions, i.e., towards the intestinal lumen and towards the blood through the lymphatic vessels in the intestinal lamina propria (28, 33). Fat feeding as well as transfection of rat IAP cDNA into Caco-2 cells increases SLP secretion (5, 6, 29), and of the two mRNAs encoding IAPs in the rat (IAP I and II), IAP II is the more active in this regard (8, 32). The murine IAP gene is the ortholog of the rat IAP II gene (21).

Despite these observations, the biological role of IAP remains to be clarified. In this report, we present evidence that mice lacking IAP show an accelerated transport of fat droplets through the intestinal wall that leads to increased body weight during high-fat feeding. Thus, IAP appears to participate in a rate-limiting step during fat absorption.

MATERIALS AND METHODS

Targeting vector. PCR was used to amplify a 1.7-kb fragment extending from the 5′ untranslated region to the beginning of exon IV and a 2.7-kb fragment encompassing intron 6 and 1.2 kb of the 3′ untranslated region of the IAP gene with genomic DNA from the D3 embryonic stem (ES) cells used for targeting. Bands of expected sizes were subcloned into the pCR2.1 vector (Invitrogen, San Diego, Calif.), and their identity was confirmed by sequencing.

A 1.7-kb *Xba*I-*Spe*I and a 2.7-kb *Not*I-*Sac*I fragment of the mouse IAP gene were then subcloned into the KS vector (Stratagene, San Diego, Calif.). The pGTN28 vector (New England Biolabs, Beverly, Mass.) was linearized with *Kpn*I, and this plasmid was blunt ended and ligated with the blunt-ended diphtheria toxin A (DTA) gene cassette obtained by *Xho*I-*Sal*I digestion of the pMC1DTA vector. The 2.7-kb *Xba*I-*Sac*I fragment was then subcloned into the DTA-pGTN28 vector, yielding the IAP-DTA-pGTN28 vector. This vector and the 1.7-kb IAP-KS vector were then cut with *Xho*I and ligated. The final construct was purified with cesium chloride ultracentrifugation and linearized with *Sca*I.

Generation of targeted ES cells and IAP KO mice. The D3 ES cells were cultured with Dulbecco modified Eagle medium supplemented with 15% fetal

* Corresponding author. Mailing address: The Burnham Institute, 10901 North Torrey Pines Rd., La Jolla, CA 92037. Phone: (858) 646-3130. Fax: (858) 713-6272. E-mail: millan@burnham.org.

† This paper is dedicated to the memory of the late Keiichi Watanabe (1934 to 2002), Tokai University, Kanagawa, Japan, for his pioneering work on IAP and for his interest and encouragement during the course of this work.

bovine serum (Tissue Culture Biologicals, Tulare, Calif.), 1% penicillin-streptomycin (Life Technologies, Rockville, Md.) with 0.1 mM nonessential amino acids (Irvine Scientific, Santa Ana, Calif.), 1 mM sodium pyruvate (Irvine Scientific), 10^{-6} M β-mercaptoethanol (Sigma, St. Louis, Mo.), 2 mM L-glutamine (Irvine Scientific), and 1,000 U of leukemia inhibition factor/ml. The D3 ES cells were electroporated with 25 μg of linearized targeting vector, seeded onto fibroblast feeders treated with mitomycin C (Sigma), and selected with 150 μg of Geneticin (Life Technologies)/ml for 2 weeks. Single clones were picked and expanded for screening and storage. Genomic DNA was extracted from the ES clones, digested with *Dra*I, separated by electrophoresis on an 0.9% agarose gel, and transferred onto Optitran (Schleicher & Schuell, Keene, N.H.). The membrane was hybridized with an internal ^{32}P-labeled probe to detect the 3.1-kb targeted and the 5.2-kb wild-type (wt) IAP allele, respectively. To further confirm the Southern blot results, PCR analysis using an external primer was also performed to amplify a 333-bp fragment of the wt IAP allele using as 5′ primer the 22-mer 5′-AGTTCAGTTCCCACATACCTGG-3′ and as 3′ primer the 22-mer 5′-CCA AACATACTGGGATCCCTAG-3′. To identify the 369-bp fragment of the targeted allele, another pair of primers was derived from the neomycin resistance gene. The 5′ primer was TGTGCTCGACGTTGTCACTGAA, and the 3′ primer was GCGGCCATTTTCCACCATGATA. The reaction conditions were 1 min at 55°C, 2 min at 72°C, and 30 s at 94°C for 35 cycles and then 1 min at 55°C and 2 min at 72°C for one cycle. Twenty microliters of each PCR product was resolved on a 1.8% agarose gel.

Two independent targeted clones with normal karyotypes were chosen for blastocyst injection. The cells were cultured in leukemia inhibitory factor-conditioned ES cell culture medium with fibroblast feeders. After two to three passages, the cells were trypsinized into a single-cell suspension and replated to eliminate the feeder cells. The cells were washed with phosphate-buffered saline and resuspended in M2 medium for injection. Both targeted clones produced chimeric founders and yielded germ line transmission of the targeted IAP allele. The targeted cells were derived from 129/Sv$^{+/+}$ mice. Chimeric founders were bred to C57BL/6 females to obtain germ line transmission. Currently the line is being maintained by sib matings.

RT-PCR and Northern blot analysis. Total mouse intestinal RNA was isolated using the Trizol reagent (Life Technologies). Reverse transcription-PCR (RT-PCR) analysis was performed using the SuperScript One-Step RT-PCR with Platinum *Taq* system kit (Life Technologies). Oligo(dT) was used for the reverse transcriptase reaction. The primers for mouse IAP were designed from the gene sequences (21). The 5′ primer had the sequence 5′-CTCATCTCCAACATGG AC-3′ and was common to both IAP and EAP. The 3′ primers were as follows: for the IAP gene, 5′-TGCTTAGCACTTTCACGG-3′; for the EAP gene, 5′-C TCTCTGTGTGTAACCAC-3′; and for the pseudo-AP, 5′-CACGATAGGCT ATGGAATC-3′. Northern blot hybridization was performed according to standard methods. Ten micrograms of total RNA isolated from the entire small intestine was loaded on each lane. The membranes were hybridized with a 569-bp *Bam*HI fragment of the IAP cDNA encompassing part of exon III through exon VI (21).

Western blot analysis. One hundred micrograms of protein was loaded on each lane of a Tris-glycine gel under denaturing and reducing conditions. An anti-mouse IAP serum was raised by immunizing a rabbit with an AP extract from Chinese hamster ovary cells stably transfected with the wt IAP gene (25). An anti-rat TNAP antiserum, displaying cross-reactivity with mouse TNAP, was a gift from Yukio Ikehara, Japan (15). Both antisera were used at a 1/1,000 dilution. Western blot analysis was done using the ECL system (Amersham, Little Chalfont, Buckinghamshire, United Kingdom).

Tissue collection, histology, and immunohistochemistry. Adult mice were sacrificed using CO_2 gas. The intestine was immediately fixed with 10% buffered formalin, washed with increasing sucrose concentrations, and embedded in OCT compound as described previously (24). Serial sections (8 μm thick) were used for immunohistochemistry and Oil Red O staining. Alternatively, some of the formalin-fixed tissues were processed through standard protocols for paraffin sections and used for hematoxylin and eosin staining. To examine IAP expression, a Vectastain ABC kit (Vector Laboratories, Burlingame, Calif.) was used according to the manufacturer's instructions. The antiserum to mouse IAP was used at a dilution of 1:500 in blocking solution and incubated with the tissue for 2 h at room temperature. Normal rabbit serum was used as the negative control. To visualize fat vesicles, after the OCT compound was removed, slides were incubated in Oil Red O solution (0.7% Oil Red O dissolved in propylene glycol) for 7 min at room temperature, washed with 85% propylene glycol and distilled water, and counterstained with hematoxylin.

Low- and high-fat diets. Gender-, age-, and genotype-matched mice (three to five in each group) were fed either a 4.5% or an 11% fat diet (Mouse Chow no. 5015; Purina Mills, St. Louis, Mo.). Body weights were monitored every 4 to 5 weeks, and the mice were observed starting at different ages (4, 6, and 9 weeks old). Observation in the long-term diet group continued for 6 to 8 months. Adult mice were also fed 500 μl of corn oil by gavage following an overnight fast. The mice were sacrificed by CO_2 gassing at various times. The intestine was immediately removed and processed as described above.

Statistics. Body weight data were obtained from 7 to 11 mice in each group at each time point. The means and standard deviations were plotted on the graph, and Student's *t* test was used to compare the statistical significance of the differences.

RESULTS

Inactivation of the IAP gene. The targeting vector used for knocking out the IAP gene is shown in Fig. 1A. This construct consisted of IAP genomic DNA spanning exon I to XI, but the neomycin resistance gene replaced exon IV to VI. Digestion of genomic DNA with the restriction enzyme *Dra*I yields a 5.2-kb fragment for the wt allele and a 3.1-kb fragment for the targeted allele. Southern blot screening demonstrated the anticipated fragments after *Dra*I digestion of genomic DNA from the targeted ES cells as well as from mouse tail genomic DNA (Fig. 1B). PCR screening also showed the anticipated 333-bp band for the wt allele and the 369-bp band for the targeted allele (Fig. 1C).

Disruption of IAP expression was confirmed by RT-PCR, Northern blotting, Western blotting, and immunohistochemistry. The 333-bp band corresponding to the wt IAP allele was detected by RT-PCR in intestinal RNA from control mice but not in IAP$^{-/-}$ mice (Fig. 1D), while expression of the syntenic EAP gene was not affected (Fig. 1D). Northern blot analysis confirmed the absence of IAP mRNA in the IAP$^{-/-}$ intestine (Fig. 1E). Mouse intestinal sections were also stained with a rabbit antiserum to mouse IAP. Positive staining was observed on the apical region of enterocytes of wt mice but not of IAP$^{-/-}$ mice (Fig. 1F). Furthermore, Western blot analysis using this same antiserum demonstrated the presence of IAP protein in the wt intestine but not in the IAP$^{-/-}$ intestine (Fig. 1G).

Phenotypic abnormalities in IAP KO mice after high-fat feeding. Despite the absence of IAP expression mice heterozygous or homozygous for the IAP null mutation did not show any abnormalities in appearance, behavior, and fertility after having been bred for several generations. Histomorphological examination of tissues revealed a similar normal appearance of all internal organs known to express IAP, including the intestine, in homozygous IAP KO mice as well as in control animals (Fig. 2A to D).

It has been hypothesized that IAP may participate in fat absorption in the intestine (20). However, no apparent fat absorption changes were observed in the IAP KO mice under a regular laboratory diet. However, abnormalities were noted in homozygous IAP KO mice fed with high-fat diets by either forced oil feeding or long-term high-fat feeding.

For forced oil feeding experiments, prefasted mice were gavaged with corn oil. The intestines were collected and fixed at various time points (ranging from 0 to 48 h) following oil feeding. Tissue sections were examined after hematoxylin-eosin staining and Oil Red O staining (Fig. 2E to H), which specifically stains fat. We observed time-dependent changes in the rate of disappearance of fat droplets in the duodenal mucosa of control and IAP$^{-/-}$ mice. At 0 h following forced

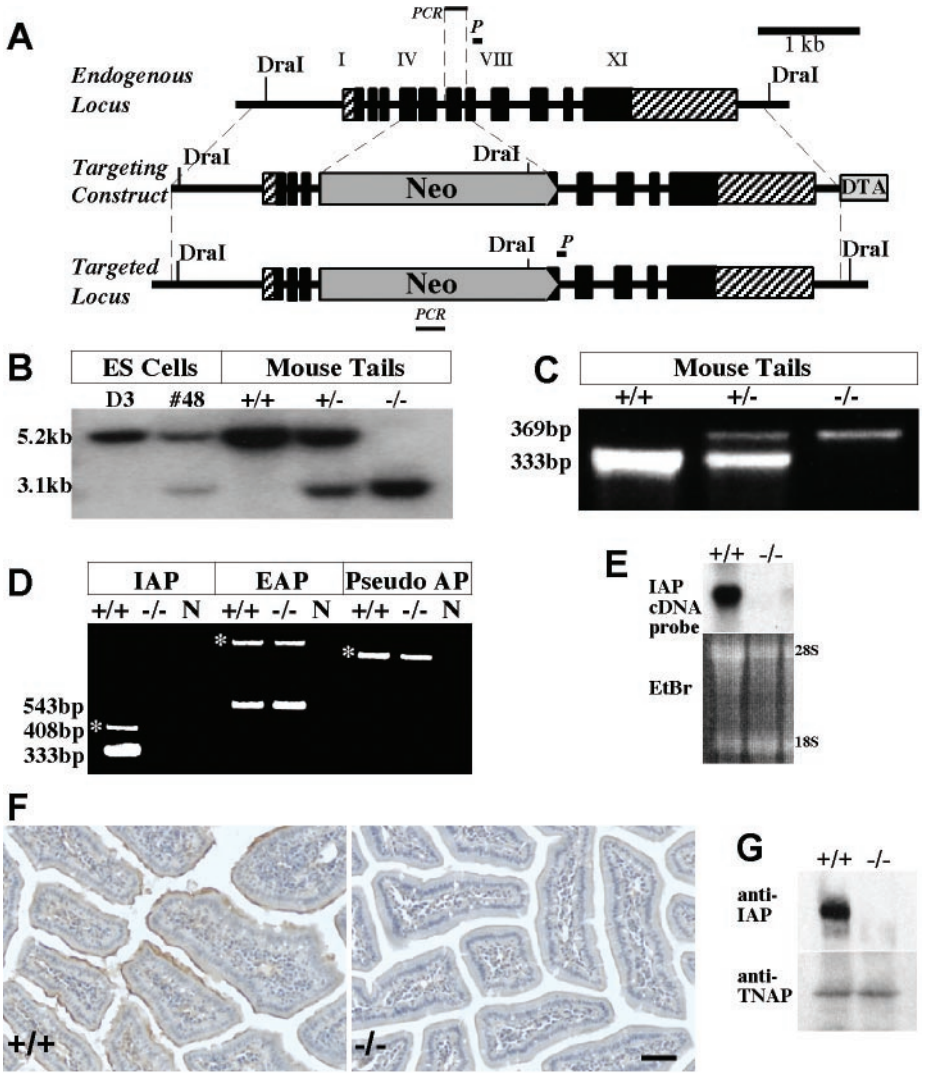

FIG. 1. Structure of the IAP targeting construct and proof of inactivation of the IAP gene. (A) The targeting construct replaced the coding regions of exon IV to VI of the IAP gene with the pGT neomycin resistance (Neo) cassette (New England Biolabs). A DTA cassette was included for negative selection. The homologous recombination events were screened by Southern blot hybridization with an internal probe (P). *Dra*I genomic DNA digestion allowed the visualization of the 3.1-kb targeted allelic fragment and the 5.2-kb wt allelic fragment. (B) Southern blot analysis of DNA derived from the targeted ES cell clone and mouse tails. D3, DNA from parental ES cells; #48, DNA from targeted ES cell clone; +/+, +/−, and −/−, tail DNA from wt, heterozygous, and homozygous mice, respectively. (C) The homologous recombination events were also confirmed by amplifying a 369-bp targeted fragment and a 333-bp wt fragment by PCR. (D) The disruption of IAP expression in the homozygous mouse intestine was confirmed by RT-PCR of total RNA from the intestine of adult control (+/+) and KO (−/−) mice. The 333-bp IAP band is not detected in IAP KO mice. The expression level of mouse EAP was unchanged in the KO mice. No transcript from the pseudogene was detected in either wt or KO mice. *, PCR products from residual genomic DNA in the RNA samples. (E) Disruption of IAP gene expression was confirmed by Northern blot hybridization with the use of a 569-bp *Bam*HI fragment of the mouse IAP cDNA as a probe. IAP transcripts were absent in the KO mice. EtBr, ethidium bromide staining for total nucleic acid. (F) Immunohistochemical localization of IAP in adult mouse duodenum. Positive signal (in brown) was observed at the apical surface of wt enterocytes but not in the corresponding regions of the IAP KO mice. Bar, 25 μm. (G) Western blot analysis detects no IAP protein in the IAP KO mouse intestines but a strong signal in the wt intestinal sample while levels of TNAP protein are unchanged in the same samples.

high-fat feeding, there was no difference between $IAP^{-/-}$ mice and wt littermate controls. Similar numbers of fat droplets were also localized at the apical region of enterocytes in $IAP^{-/-}$ and wt mice 3 h after fat feeding. However, 5 h after feeding, fat droplets were no longer observable in $IAP^{-/-}$ mice while they were still present in significant numbers in the enterocytes of wt mice. This apparent accelerated transport of lipids through the intestine of $IAP^{-/-}$ mice is accompanied by an elevation in plasma triglyceride levels 7 h after gavage (Fig. 3A).

For long-term high-fat feeding, we fed $IAP^{-/-}$ and wt control mice either a normal 4.5% fat or an 11% fat mouse chow. wt mice fed a regular-fat diet revealed a consistent difference in body weight gain between males and females (Fig. 3B). Long-term observation showed a different rate of weight increase for IAP KO versus control mice when fed a high-fat diet

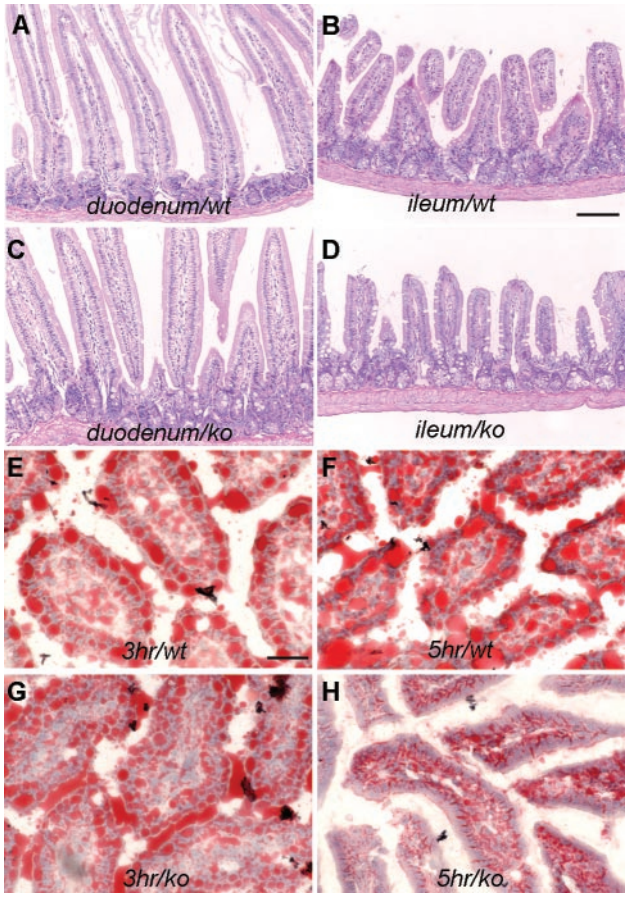

FIG. 2. Histochemical analysis of wt and IAP KO intestines. (A to D) Hematoxylin and eosin staining of sections of duodenum and ileum from wt and IAP KO mice. No morphological difference was observed in the duodenum, jejunum, or ileum of IAP KO mice. Bar, 100 μm. (E to H) Oil Red O staining, specific for lipid, of duodenum sections from wt and IAP KO mice to visualize lipid droplets in red. Lipid droplets in the duodenum of IAP KO mice subjected to forced feeding with oil are indistinguishable from those of wt controls after 3 h of incubation; however, after 5 h of incubation the enterocytes in the IAP KO mice contained fewer lipid droplets (H), while the droplets were still present in the wt mice (F). Bar, 30 μm.

from 4 weeks of age (Fig. 3C). This response was observed in both male and female IAP KO mice but was much more dominant in males as expected from the relative difference in weight as shown in Fig. 3B. Furthermore, this increase in body weight was not dependent on the time at which the high-fat diet was initiated, as similar curves were obtained if high-fat feeding began at 4, 6, or 9 weeks of age. Figure 3D shows the relative difference in size achieved by a wt and an $IAP^{-/-}$ mouse at 30 weeks of age under a high-fat diet.

DISCUSSION

IAP is a glycosylphosphatidylinositol-anchored enzyme expressed mainly in the microvillus membrane of the intestine. In the rat, 1 to 2% of IAP is secreted into the circulation and gastrointestinal lumen (27). The enzyme that is secreted basolaterally is free of glycosylphosphatidylinositol linkage (4), but the luminal IAP is membrane bound. The luminal membrane is different from the microvillus membrane and does not represent sloughed membrane as in the calf but represents a distinct organelle with surfactant-like activity. This secreted membrane, enriched in dipalmitoyl-phosphatidylcholine, has been designated SLP.

SLP is produced by the enterocyte and appears to be involved in fat absorption (1). In the rat, either force-feeding of corn oil (5) or natural feeding of a high-fat diet to the suckling animal (6) increases IAP and SLP secretion. IAP is found on intracellular membranes that are associated with the lipid droplets in the enterocyte of suckling rats (6). Transfection of the rat IAP cDNA enhances the production and secretion of IAP and SLP in cultured cells (29). Thus, IAP could be involved in production or function of SLP either directly or indirectly. In addition, when chylomicron secretion is blocked in adult rats by feeding them the detergent Pluronic L-81, membranes are retained within the enterocyte, and these membranes are enriched in IAP as detected by immunoelectron microscopy (18). However, the intracellular retention was implied morphologically by retention of fat globules with surrounding membranes and by a fall in secreted SLP level. Upon quantification, only a small albeit statistically significant change in SLP numbers could be detected. These data were interpreted initially as suggesting that SLP enhanced fat absorption. The data from the present paper, however, suggest an alternative explanation, i.e., that SLP and IAP are involved in the transcytotic movement of lipid droplets following a meal, but that they slow it down (and perhaps direct it), possibly by protein-protein interactions.

What are the data that suggest that IAP and/or SLP might be involved in transcytosis? First, IAP binds to other proteins, including serum immunoglobulin G (27), enterocyte calbindin (17), and the hepatic asialoglycoprotein receptor (23). No direct assessment of IAP binding to intracellular proteins has been made to date. Second, SLP contains other proteins, including one known to be involved in transcytosis, i.e., cubilin (19). IAP and cubilin are present not only in SLP isolated from the luminal surface of the cell, as in all the studies reported previously, but also in intracellular SLP. After fat feeding, both cubilin and IAP colocalized to the intracellular regions surrounding lipid droplets (19). Third, these recent studies have also confirmed the existence of a membrane surrounding the intracellular lipid droplet in the rat. Thus, SLP appears to surround the lipid droplet and contains proteins that could modify the movement of the lipid droplet through the cell.

Our present data provide support for the studies that suggested a role for SLP and IAP in fat absorption. Indeed, the IAP KO model was created to test the hypothesis that these factors were related to fat absorption. The original hypothesis (that IAP and/or SLP was essential for transcytosis) appears to be proven incorrect by the results of this study, but the fact that IAP and SLP play a role has been confirmed. As noted above, none of the data obtained to date are inconsistent with the revised hypothesis, i.e., that IAP and/or other SLP components bind to intracellular proteins and retard the movement of the fat droplet across the enterocyte. The role of IAP in decreasing the rate of fat absorption could be viewed as logical for animals that ingest high-fat diets. The activity of AP increases steadily from the level in the blind eel to the highest level in mammals,

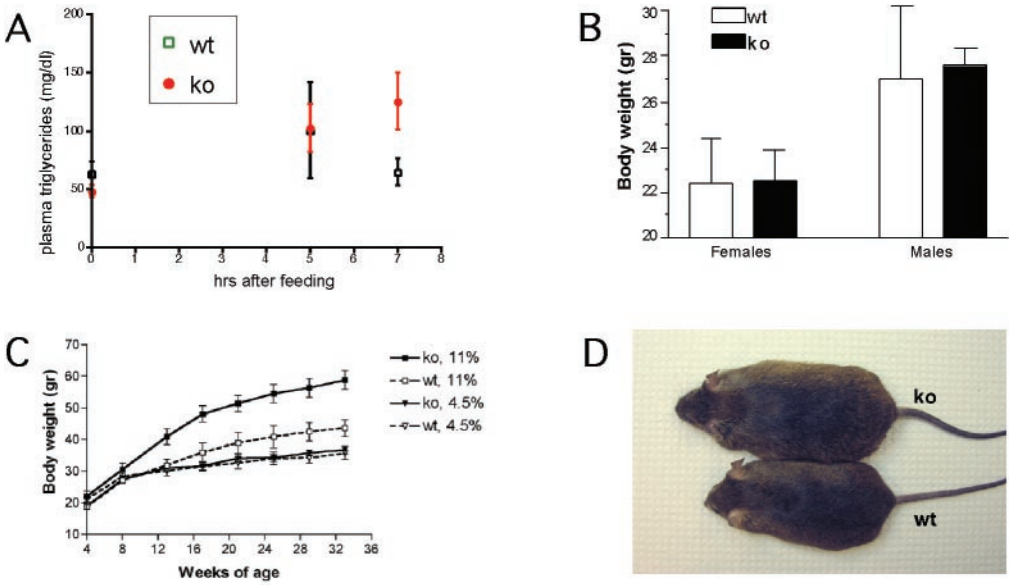

FIG. 3. Plasma triglyceride levels and body weights of control and IAP KO mice under different feeding conditions. (A) Triglyceride levels in plasma from the mice subjected to forced oil feeding were measured at 0, 5, and 7 h following gavage. After 7 h the triglyceride levels were significantly higher in IAP KO mice than in wt controls. (B) Body weights of IAP KO (ko) and control wt mice at 8 weeks of age fed a regular diet containing 4.5% fat were measured, and average values were obtained from 7 to 11 mice in each group. The body weights of male mice are higher than those of female mice among both KO and control mice; however, there is no statistical difference between the control and the IAP KO mice subjected to a regular diet. (C) Body weights of control and IAP KO male mice under a regular-fat diet (4.5%) or high-fat diet (11%) feeding regimen initiated at 4 weeks of age. There is a clear difference between the weight gain in IAP KO mice subjected to the high-fat diet and that in the control mice. (D) Example of the difference in body size at 30 weeks of age between IAP KO and wt male mice fed long-term with a high-fat diet.

and the properties that are characteristic of the IAP isozyme were established late in evolution and only in mammals (16).

ACKNOWLEDGMENTS

This work was supported by grant CA 42595 from the National Institutes of Health.

S. Narisawa and L. Huang contributed equally to the work.

REFERENCES

1. **Alpers, D. H., M. J. Engle, and R. Eliakim.** 2000. The possible role of intestinal surfactant-like particles in the absorption of triacylglycerols in the rat, p. 325–334. *In* C. M. Mansbach II, P. Tso, and A. Kuksis (ed.), Intestinal lipid metabolism. Kluwer Academic, New York, N.Y.
2. **Dehghani, H., S. Narisawa, J. L. Millán, and A. C. Hahnel.** 2000. Effects of disruption of the embryonic alkaline phosphatase gene on the preimplantation development of the mouse. Dev. Dyn. **217:**440–448.
3. **Eliakim, R., K. DeSchryver-Kecskemeti, L. Nogee, W. F. Stenson, and D. H. Alpers.** 1989. Isolation and characterization of a small intestinal surfactant-like particle containing alkaline phosphatase and other digestive enzymes. J. Biol. Chem. **264:**20614–20619.
4. **Eliakim, R., M. J. Becich, K. Green, and D. H. Alpers.** 1990. Both tissue and serum phospholipases release rat intestinal alkaline phosphatase. Am. J. Physiol. **259:**G618–G625.
5. **Eliakim, R., A. Mahmood, and D. H. Alpers.** 1991. Rat intestinal alkaline phosphatase secretion into lumen and serum is coordinately regulated. Biochim. Biophys. Acta **1091:**1–8.
6. **Eliakim, R., M. J. Becich, K. Green, and D. H. Alpers.** 1991. The developmental expression of intestinal surfactant-like particles in the rat. Am. J. Physiol. **261:**G269–G279.
7. **Eliakim, R., G. S. Goetz, S. Rubio, B. Chailley-Heu, J. S. Shao, R. Ducroc, and D. H. Alpers.** 1997. Isolation and characterization of surfactant-like particles in rat and human colon. Am. J. Physiol. **272:**G425–G434.
8. **Engle, M. J., and D. H. Alpers.** 1992. The two mRNAs encoding rat intestinal alkaline phosphatase represent two unique nucleotide sequences. Clin. Chem. **38:**2506–2509.
9. **Fedde, K. N., L. Blair, J. Silverstein, R. S. Weinstein, K. Waymire, G. R. MacGregor, S. Narisawa, J. L Millán, and M. P. Whyte.** 1999. Alkaline phosphatase knock-out mice recapitulate the metabolic and skeletal defects of infantile hypophosphatasia. J. Bone Miner. Res. **14:**2015–2026.
10. **Glickman, R. M., D. H. Alpers, G. D. Drummey, and K. J. Isselbacher.** 1970. Increased lymph alkaline phosphatase after fat feeding: effects of medium chain triglycerides and inhibition of protein synthesis. Biochim. Biophys. Acta **201:**226–235.
11. **Hahnel, A. C., D. A. Rappolee, J. L. Millán, T. Manes, C. A. Ziomek, N. G. Theodosiou, Z. Werb, R. A. Pedersen, and G. A. Schultz.** 1990. Two alkaline phosphatase genes are expressed during early development in the mouse embryo. Development **110:**555–564.
12. **Harris, H.** 1989. The human alkaline phosphatases: what we know and we don't know. Clin. Chim. Acta **186:**133–150.
13. **Hessle, L., K. A. Johnsson, H. C. Anderson, S. Narisawa, A. Sali, J. W. Goding, R. Terkeltaub, and J. L Millán.** 2002. Tissue-nonspecific alkaline phosphatase and plasma cell membrane glycoprotein-1 are central antagonistic regulators of bone mineralization. Proc. Natl. Acad. Sci. USA **99:**9445–9449.
14. **Hietanen, E.** 1973. Interspecific variation in the levels of intestinal alkaline phosphatase, adenosine triphosphatase and disaccharidases. Comp. Biochem. Physiol. **46A:**359–369.
15. **Hoshi, K., N. Amizuka, K. Oda, Y. Ikehara, and H. Ozawa.** 1997. Immunolocalization of tissue non-specific alkaline phosphatase in mice. Histochem. Cell Biol. **107:**183–191.
16. **Komoda, T., I. Koyama, A. Nagata, Y. Sakagishi, K. DeSchryver-Kecskemeti, and D. H. Alpers.** 1986. Ontogenic and phylogenic studies of intestinal, hepatic, and placental alkaline phosphatase. Evidence that intestinal alkaline phosphatase is a late evolutionary development. Gastroenterology **91:**277–286.
17. **Leathers, V. L., and A. W. Norman.** 1993. Evidence for calcium mediated conformational changes in calbindin-D28K (the vitamin D-induced calcium binding protein) interactions with chick intestinal brush border membrane alkaline phosphatase as studied via photoaffinity labeling techniques. J. Cell Biochem. **52:**243–252.
18. **Mahmood, A., F. Yamagishi, R. Eliakim, K. DeSchryver-Kecskemeti, T. L. Gramlich, and D. H. Alpers.** 1994. A possible role for rat intestinal surfactant-like particles in transepithelial triacylglycerol transport. J. Clin. Investig. **93:**70–80.
19. **Mahmood, A., J. Shao, and D. H. Alpers.** 2003. Rat enterocytes secrete surfactant-like particles containing alkaline phosphatase and cubilin in response to corn oil feeding. Am. J. Physiol. Gastrointest. Liver Physiol. **285:** G433–G441.
20. **Malagelada, J. R., L. L. Stolbach, and W. G. Linscheer.** 1977. Influence of

carbon chain length of dietary fat on intestinal alkaline phosphatase in chylous ascites. Am. J. Dig. Dis. **22:**629–632.
21. **Manes, T., K. Glade, C. A. Ziomek, and J. L. Millán.** 1990. Genomic structure and comparison of mouse tissue-specific alkaline phosphatase genes. Genomics **8:**541–554.
22. **McComb, R. B., G. N. Bowers, and S. Posen.** 1979. Alkaline phosphatase. Plenum Press, New York, N.Y.
23. **Meijer, D. K., H. B. Scholtens, and M. J. Hardonk.** 1982. The role of the liver in clearance of glycoproteins from the general circulation, with special reference to intestinal alkaline phosphatase. Pharm. Weekbl. Sci. **4:**57–70.
24. **Narisawa, S., N. Fröhlander, and J. L. Millán.** 1997. Inactivation of two mouse alkaline phosphatase genes and establishment of a model of infantile hypophosphatasia. Dev. Dyn. **208:**432–446.
25. **Narisawa, S., M. C. Hofmann, C. A. Ziomek, and J. L. Millán.** 1992. Embryonic alkaline phosphatase is expressed at M-phase in the spermatogenic lineage of the mouse. Development **116:**159–165.
26. **Narisawa, S., C. Wennberg, and J. L. Millán.** 2001. Abnormal vitamin B6 metabolism in alkaline phosphatase knock-out mice causes multiple abnormalities, but not the impaired bone mineralization. J. Pathol. **193:**125–133.
27. **Shinozaki, T., H. Watanabe, K. Takagishi, and K. P. Pritzker.** 1998. Allotype immunoglobulin enhances alkaline phosphatase activity: implications for the inflammatory response. J. Lab. Clin. Med. **132:**320–328.
28. **Sussman, N. L., R. Eliakim, D. Rubin, D. H. Perlmutter, K. DeSchryver-Kecskemeti, and D. H. Alpers.** 1989. Intestinal alkaline phosphatase is secreted bidirectionally from villous enterocytes. Am. J. Physiol. **257:**G14–G23.
29. **Tietze, C. C., M. J. Becich, M. Engle, W. F. Stenson, R. Eliakim, and D. H. Alpers.** 1992. Caco-2 cell transfection by rat intestinal alkaline phosphatase cDNA increases surfactant-like particles. Am. J. Physiol. **263:**G756–G766.
30. **Waymire, K. G., J. D. Mahuren, J. M. Jaje, T. R. Guilarte, S. P. Coburn, and G. R. MacGregor.** 1995. Mice lacking tissue non-specific alkaline phosphatase die from seizures due to defective metabolism of vitamin B-6. Nat. Genet. **11:**45–51.
31. **Xie, Q. M., Y. Zhang, S. Mahmood, and D. H. Alpers.** 1997. Rat intestinal alkaline phosphatase II messenger RNA is present in duodenal crypt and villus cells. Gastroenterology **112:**376–386.
32. **Xie, Q., and D. H. Alpers.** 2000. The two isozymes of rat intestinal alkaline phosphatase are products of two distinct genes. Physiol. Genomics **3:**1–8.
33. **Yamagishi, F., T. Komoda., and D. H. Alpers.** 1994. Secretion and distribution of rat intestinal surfactant-like particles after fat feeding. Am. J. Physiol. **266:**G944–G952.